Mechanical Systems and Signal Processing 182 (2023) 109583

Contents lists available at ScienceDirect

Mechanical Systems and Signal Processing

journal homepage: www.elsevier.com/locate/ymssp

Non-intrusive determination of shock absorber characteristic curves by means of evolutionary algorithms

E. Carabias, J.A. Cabrera *, J.J. Castillo, J. Pérez, M. Alcázar

Mechanical Engenieering Department, University of Málaga, C/ Doctor Ortiz Ramos, s/n. 29071 Málaga, USA

ARTICLE INFO

Communicated by Yaguo Lei

Keywords:
Suspension fault detection
Damper characteristic curve
Tyre model
Evolutionary algorithms

ABSTRACT

The fault detection in the components of the suspension system of road vehicles is of great importance. The optimal performance of the suspension system has a big influence on the safety and stability of a vehicle. Vehicle inspection services make use of different methods of fault diagnosis of shock absorbers without the need to remove them from the vehicle. These methods generally provide an average value of the damping coefficient or a value related to the efficiency of the damper. Next, acceptance or rejection criteria are used to evaluate the condition of the damper. Consequently, there is currently no objective criterion for detecting the malfunctioning or faulty condition of shock absorbers. In this work, a novel methodology capable of obtaining the complete force–velocity characteristic curve of the shock absorber is proposed. For this purpose, the importance of using an appropriate tyre model to obtain the suspension parameters is first studied. In addition, the displacements of the sprung and unsprung masses and the excitation of the system are obtained experimentally. Next, the points that model the complete characteristic curve of a shock absorber are obtained by means of an optimization method based on evolutionary algorithms. Real tests have been conducted on a complete vehicle suspension test bench to verify the effectiveness of the proposed methodology.

1. Introduction

The suspension system of road vehicles is of fundamental importance for the safety and comfort of passengers. The presence of defects in the suspension components is related to vehicle stability problems and degradation of handling performance. The shock absorber is one of the main components of the suspension system. The main function of the shock absorber is to dissipate energy, which contributes to isolating the vehicle body from excessive vibrations and movements induced in the road-wheel interaction. Furthermore, shock absorbers also reduce the loss of contact between the tyre and road, especially on bumpy or rough roads. In short, the suspension system works as a filter for the vehicle's body movements at frequencies that would otherwise cause discomfort to the vehicle's passengers or that would compromise the safety of the vehicle. For this reason, knowledge of damper performance is of utmost importance in vehicle dynamics.

The loss of the effectiveness of the shock absorber due to its malfunction can affect the stability and safety of a vehicle [1–6]. Hence, many research groups have tried to develop vehicle dynamics models in which the suspension systems behaviour is reproduced as precisely as possible. The most widely used suspension models take into account the connection of the sprung and unsprung masses by means of a spring-shock absorber system, typically using an elastic stiffness and a constant damping coefficient. Some also model the

* Corresponding author.
E-mail address: jcabrera@uma.es (J.A. Cabrera).

https://doi.org/10.1016/j.ymssp.2022.109583
Received 4 March 2022; Received in revised form 13 July 2022; Accepted 15 July 2022
Available online 20 July 2022

contact between the tyre and road, most of them using a linear tyre stiffness [7–9]. This way, an approximate vertical vehicle behaviour model is obtained. However, if more accuracy is required, a more realistic tyre-road contact model and a closer-to-reality modelling of shock absorber behaviour, making use of its response characteristic curves, are needed. In their work, Simms and Crolla [10] reported significant discrepancies in the output of a quarter-vehicle model in different driving situations if a constant damping coefficient or the real characteristic curve of the damper were used.

Obtaining these characteristic parameters used in suspension models can become complex if shock absorbers are not disassembled from the vehicle and tested on specific benches. For example, to obtain the characteristic curves of dampers, test benches are used that excite the damper over the entire frequency range to provide the force–velocity and force–displacement curves [10–11]. These curves are not linear and show different behaviour when the shock absorber is compressed or extended or when the inter-chamber valves are opened. Test benches are also used for the vertical characterization of tyres [12–13]. Many of these works focus on obtaining a vertical model of tyres, concluding that many factors influence their behaviour, such as the appearance of viscoelastic and hysteresis phenomena. These factors can affect the behaviour of suspension systems in vehicles if they are not taken into account.

All the aforementioned systems are necessary for the accurate modelling of suspension systems of vehicles and for the detection of failures in shock absorbers. Nevertheless, these methods require the disassembly of each of the suspension elements and the use of devices or benches for their characterization. There is another line of research that focuses on determining suspension parameters without the need of dismounting its components. To do so, they propose the use of test benches where the complete suspension system of a vehicle can be tested or they resort to sensorized vehicles.

In this sense, one of the simplest methods is the one developed by Lajki et al. [14], where the distance between the sprung mass and the wheel center of the vehicle and the vertical force in the contact between the tyre and road are measured. With these values, and by solving a quarter-vehicle system with one degree of freedom, the spring stiffness and the shock absorber damping coefficient are obtained. This approach is easy to apply and no special equipment is required to conduct the tests. However, the main drawback lies in the fact that the calculated damping constant is approximate and does not take into account the characteristic curve of a shock absorber, which is not symmetrical in compression and extension and varies depending on the velocity. In addition, in the experimental tests that were carried out, the system was not excited enough. Therefore, the complete damping curve cannot be obtained. Furthermore, the model used does not take the tyre into account either, which reduces the accuracy of the calculation of the damping coefficient. Nozaki and Inagaki [15] also excited the vehicle body to obtain a damping coefficient, using a quarter-vehicle model. A more sophisticated method was developed by Isermann [16] and Fischer and Isermann [17]. They proposed a method that estimates the suspension parameters using a Recursive Least Squares (RLS) or Discrete Square Root Filtering in Information (DSFI) algorithm. To this end, they linked the unsprung and sprung masses of a quarter-vehicle model with a spring-damper system and modelled the contact between the tyre and road with constant stiffness. Next, a quarter car test bench that can excite the suspension system in a wide range of movements and frequencies was used to check the estimation algorithm robustness. It is observed how the algorithm estimates the curves by linearizing them in a specific number of parts, thus obtaining different kinds of behaviour in the extension and compression movements of the shock absorber. The estimation algorithm was also tested in a real vehicle. In this case, only one damping curve is obtained with two characteristic values: a constant damping for extension and another one for compression. This is due to the fact that the excitation of the system does not cover all frequency ranges. Schiehlen and Hu [18] proposed the use of a hardware-in-the-loop system for the identification of the response of shock absorbers. They resorted to a stochastic model to simulate the roughness of the road and, consequently, the excitation of the system. The HiL system consisted of a quarter model of a vehicle and a suspension bench where the real behaviour of the shock absorber was obtained. The damper characteristic curves were linearized in sections and modelled with five parameters, which were obtained by correlation-based methods. Calvo [19–20] also proposed a method for estimating the damper ratio, thereby establishing a criterion to determine if a damper works properly. In this method, a platform test rig is used to excite the system at a frequency of up to 25 Hz. The force and displacement on the platform that excites the vehicle tyre are measured. With these values, the transfer function of the system in frequency is obtained. Subsequently, the damping ratio of the first vibration mode (the so-called sprung mass mode) is estimated. As in previous methods, a constant value of the damping coefficient is obtained and the complete characteristic curve of the damper cannot be provided. This value is used to determine the shock absorber condition. Thus, the authors indicate a range in the damper ratio in which a rejection criterion can be established for the inspection of shock absorbers in vehicles. Finally, Klapka et al. [21] studied and classified all the existing methods for determining the conditions of shock absorbers in vehicle inspections, some of which have been previously described. All the methods used in vehicle inspections provide a constant parameter related to the whole suspension system condition. Next, acceptance or rejection criteria are applied to decide the result of the inspection. These authors recommend the use of the damper ratio as the key parameter to determine the acceptance or not of the suspension system in a vehicle and describe five possible ways of estimating it. They also conclude that whether the determination of the damper ratio is based on a linear model of a quarter of a vehicle, the non-linearities existing in the suspension systems can affect the accuracy of the obtained values.

Therefore, the methods used to estimate parameters in suspension systems without removing them from the vehicle have the following characteristics:

- Most estimation methods use a constant average parameter to model the characteristic curves of the dampers.
- The excitation of the system is not sufficient to reach the speeds necessary to model the characteristic curve of the damper completely.
- All of them use a quarter or half-vehicle model where the tyre is modelled by constant stiffness. This way, effects such as viscoelasticity and hysteresis are not taken into account.

- No method models the non-linearities existing in the tyre and in the characteristic curves of the shock absorbers and the influence of other suspension components, such as silent blocks and, anti-roll bars.

This work aims to study all the weaknesses of the methods mentioned above and to propose a new methodology capable of solving them. To this end, a single-point tyre model is incorporated into a quarter car vehicle model. For this purpose, the Maxwell tyre model is used to take into account tyre viscoelastic behaviour [22–23]. Next, the influence of tyre modelling on the determination of the parameters that define the suspension system is evaluated. To achieve this objective, a 2GDL quarter-vehicle suspension test bench [12] will be used. This test bench allows estimating the error between the experimental characteristic curves and the damper ratio obtained with the aforementioned approaches. Once the influence of tyre modelling has been evaluated, a full vehicle model and the measurement of the displacements of the sprung and unsprung masses in a test with a real vehicle will be used to determine the suspension characteristic curves. The characteristic curves in shock absorbers will be obtained by means of an optimization process using genetic algorithms. Hence, the robustness of a system that is capable of obtaining the suspension parameters and the characteristic curves of the shock absorber without having to disassemble any component of the vehicle is validated.

This paper has been structured as follows. In the 'Influence of the tyre model on obtaining the parameters of the suspension' section, the study of the influence of tyre modelling on the accuracy of the determination of the shock absorber characteristic curve is described. Furthermore, the use of the damping coefficient to evaluate the condition of the suspension system is studied in section 3. Next, the proposed methodology to obtain the characteristic curves is evaluated by means of real tests in the 'Experimental determination of the suspension parameters on a vehicle' section. Finally, the main contributions of this research are summarized in the 'Conclusion' section.

2. Influence of the tyre model on obtaining the parameters of the suspension

A quarter-vehicle model is used to study the influence of the tyre on the dynamic models of vehicle suspension systems (Fig. 1). This model allows obtaining the characteristic curves of the suspension system through tests conducted on a suspension bench that has been developed by this research group [12]. The dynamic quarter-vehicle model is defined according to the following equations:

$$M_s \bullet \ddot{x}_s + C_a \bullet \left(\dot{x}_s - \dot{x}_t\right) + K_a \bullet (x_s - x_t) = 0 \tag{1}$$

$$M_u \bullet \ddot{x}_t - C_a \bullet \left(\dot{x}_s - \dot{x}_t\right) - K_a \bullet (x_s - x_t) + f_v + K_s \bullet (x_t - x_r) = 0 \tag{2}$$

Where the value of f_v is defined by the following differential equation:

$$\frac{C_d}{K_d} \bullet \dot{f}_v + f_v = C_d \bullet \left(\dot{x}_t - \dot{x}_r\right) \tag{3}$$

Differential equation (3) can be transformed into an ordinary equation by applying the finite difference method. Thus, the following expression is obtained:

$$f_v(t) = \frac{C_d}{1+\gamma} \bullet \left(\dot{x}_t - \dot{x}_r\right) + \vartheta \bullet f_v(t-1) \tag{4}$$

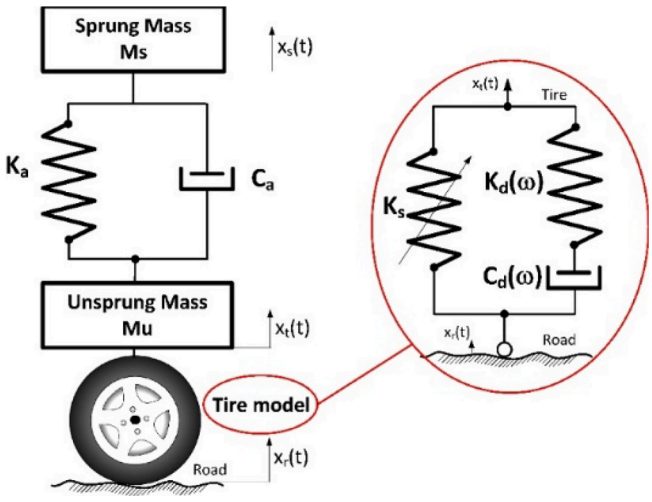

Fig. 1. Dynamic model of a quarter vehicle.

Where:

$$\gamma = \frac{C_d}{K_d \bullet \Delta t}$$
$$\vartheta = \frac{\gamma}{1+\gamma}, C_\gamma = \frac{C_d}{1+\gamma} \tag{5}$$

Equations (1), (2) and (4) have the following parameters that can be calculated directly: K_s (tyre stiffness), K_a (suspension spring stiffness) and ϑ (viscoelastic coefficient). The parameters that will be estimated are M_s (suspended mass), M_u (unsprung mass), C_a (shock absorber characteristic curve) and C_d (tyre damping). In addition, x_s (displacement of the suspended mass), x_t (displacement of the unsprung mass) and x_r (excitation displacement of the system) will also be measured.

Once the dynamic model of the vehicle has been established, tests are conducted on a quarter car test bench. In this model, x_s, x_t and , x_r are the displacements of the sprung mass, unsprung mass, and test plate respectively, which can be measured on this test bench. Excitation x_r is a sinusoidal movement with a frequency range from 0 to 20 Hz with an amplitude limited up to $\pm$ 4 mm to avoid contact loss between the tyre and bench plate. With the data of the measurements at each instant of time, a process of identification of the remaining parameters is carried out by means of genetic algorithms. To do so, an algorithm objective function is required and the parameters that need to be estimated are defined. The problem to be solved is outlined in Fig. 2. It is formulated mathematically as follows:

$$f_1(\chi, \tau_i) \equiv \chi(1) \bullet \ddot{x}_s(\tau_i) + \chi(4..24) \bullet v_i + K_a \bullet \zeta_i = 0 \tag{6}$$

$$f_2(\chi, \tau_i) \equiv \chi(2) \bullet \ddot{x}_t(\tau_i) - \chi(4..24) \bullet v_i - K_a \bullet \zeta_i + f_v(\chi(3), \vartheta, \tau_i) + K_s \bullet \varsigma_i = 0 \tag{7}$$

$$\begin{aligned} &where: \\ &\chi = \left\{M_s, M_u, C_d, C_a^1 \cdots, C_a^{20}\right\} \\ &v_i = \dot{x}_s(\tau_i) - \dot{x}_t(\tau_i) \\ &\zeta_i = x_s(\tau_i) - x_t(\tau_i) \\ &\varsigma_i = x_t(\tau_i) - x_r(\tau_i) \\ &\tau_i = t_o + i \bullet \Delta t \end{aligned} \tag{8}$$

$$GF = min\left[\sum_{i=0}^{nsample} \frac{\sqrt{\left\{f_1(\chi,\tau_i)^2 + f_2(\chi,\tau_i)^2\right\}}}{nsample}\right]$$
$$subjectto: \chi(1) + \chi(2) = M_{1/4} \tag{9}$$

Equation (9) defines the optimization problem, where f_1 and f_2 are the components of the goal function to be minimized, obtained from equations (1) and (2), v_i and ζ_i are the speed and displacement differences between the sprung and unsprung masses, ς_i is the

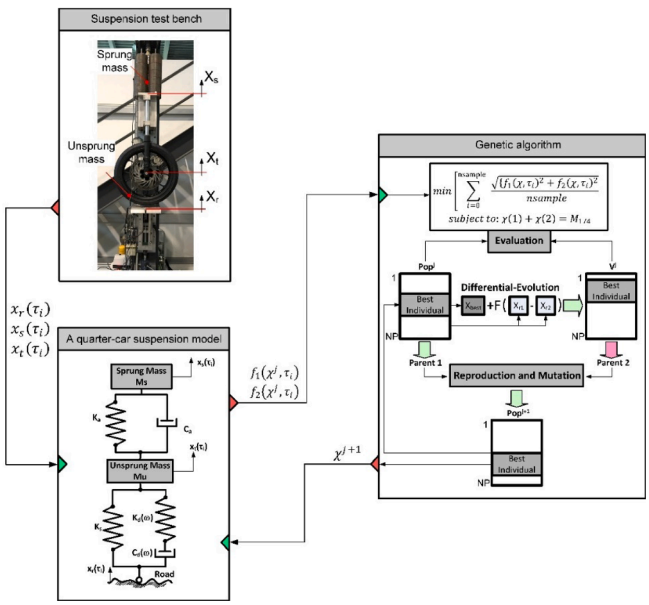

Fig. 2. Methodology for estimating suspension parameters.

displacement difference between the unsprung mass and test plate, χ is the vector of variables to be estimated and *GF* is the goal function. Solutions were obtained at time τ_i, with time step $\Delta t = 0.001$ s, i being the number of samples. The known parameters of the model are defined in Table 1. The optimization algorithm uses the evolution of a population of individuals formed by the vector of variables by means of the paradigm called Differential Evolution that this research group has already used with success in other engineering problems [24]. In this paper, genetic algorithms have been used as a tool to solve the optimization problem. The main advantages of these methods are their simplicity in implementing the algorithms and their low computational cost in some cases. The differential evolution-based genetic algorithm used in this paper is considered to be appropriate for this approach since it provides reasonably good solutions to the optimization problems in a quick manner without requiring deep knowledge of the search space.The process is the following: first, a test is conducted on the test bench. The position, velocities and accelerations of the plate, sprung and unsprung masses are recorded. Next, the optimization algorithm searches the vector of variables that minimizes the goal function taking into account all the samples.

To evaluate the performance of the proposed strategy, a series of tests on a motorcycle front suspension was carried out. These tests allowed determining the stiffness of the tyre and the fork spring. This task was done without disassembling the suspension components. The stiffness curves are shown in Fig. 3. As it can be seen, the curves are not linear. However, the spring and tyre stiffnesses can be considered linear in the working range according to the test results (red line). For this reason, fork stiffness K_s and tyre stiffness K_a have been modelled with a constant value in Table 1.

Among the variables to be identified in vector χ, viscoelastic coefficient ϑ should be highlighted. This coefficient has previously been studied by our research group [12]. The following conclusions were drawn:

- In tests carried out on two completely different tyres, a 90/58 R17 size motorcycle tyre and a 205/65 R15 size passenger car tyre, stiffness K_d and damping C_d of the tyres vary when the tyres are tested at different excitation frequencies (Fig. 4a, 4c).
- On the other hand, the viscoelastic coefficient, defined as $\vartheta = \gamma/1 + \gamma$, remains almost constant when the excitation frequency and load vary (Fig. 4b, 4d).

This last conclusion makes it easier to calculate the viscoelastic coefficient of a tyre, since it does not depend on the excitation frequency and tyre load. Furthermore, it can be considered constant, independently of the tyre. On the other hand, the damping coefficient of tyre C_d depends on the load and excitation frequency. However, in order to avoid introducing two new frequency-dependent parameters in the optimization process, the research group has studied the influence of this parameter in obtaining the shock absorber characteristic curve. As you can see in Fig. 4a and 4c, the C_d value remains stable for excitation frequencies above 5 Hz in two different tyres. In addition, to calculate viscoelastic force f_v (equation (4)), we need viscoelastic coefficient ϑ and the $C_\gamma = C_d/(1+\gamma)$ parameter. This last parameter depends on damping coefficient C_d and the $\gamma \gg 1$ parameter, which is dimensionless. Consequently, in this work, a constant mean value of tyre damping C_d will be considered. This assumption is valid since the committed error is low due to its stable value for high tyre excitation frequencies and because the γ parameter makes ratio $C_d/(1+\gamma)$ more enclosed.

Regarding the parameters necessary to model the shock absorber characteristic curve, the maximum and minimum excitation velocities of the shock absorbers have been determined in this work. Next, this range of velocities has been split into 20 calculation points, obtaining the damper force in each of them. This identifies 20 points on the force–velocity characteristic curve of the shock absorber. These points define values $\{C_a^1 \cdots C_a^{20}\}$ of the vector of variables χ (see Fig. 5).

Once the points have been obtained, they are fitted to a hyperbolic tangent curve model [25] with four parameters (equation (8)). This curve reproduces the shock absorber characteristic curve.

$$f_a = c_s \bullet v + \kappa \bullet \{tanh(\mu \bullet v + \beta) - tanh(\beta)\} \tag{10}$$

Table 1
Model and optimization algorithm parameters.

Model constant	Description	Value
K_s	Suspension stiffness	14040 N/m
K_a	Tyre stiffness	101018 N/m
ϑ	Viscoelastic coefficient	0.97
C_γ	Velocity coefficient	55 Ns/m
$M_{1/4}$	Vehicle mass (1/4)	109.3 Kg
Δt	Sample time	1 ms
Algorithm parameters	**Description**	**Value**
F	Disturbance factor	1
CP	Crossover probability	0.3
MP	Mutation probability	0.1
NP	Number of individuals	70
j	Number of iterations	3000
nsample	Number of samples	5000

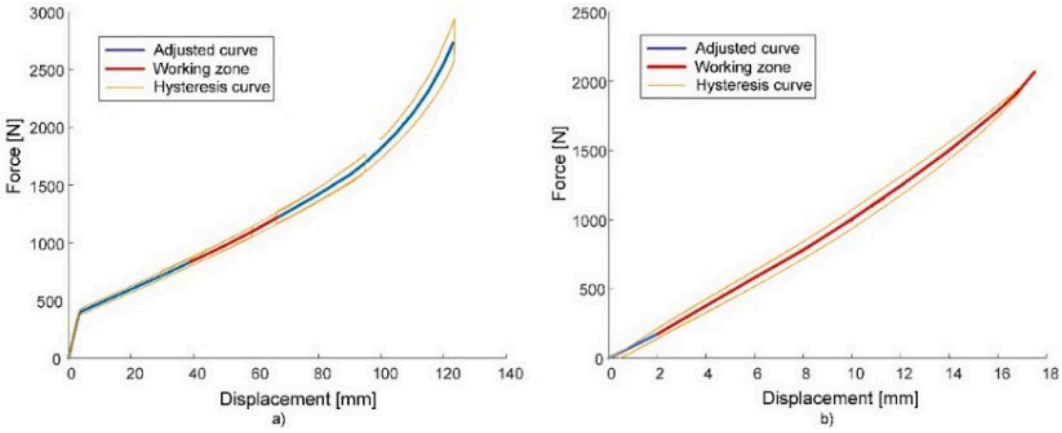

Fig. 3. Stiffness curves. a) Stiffness of the suspension spring. b) Stiffness of the tyre.

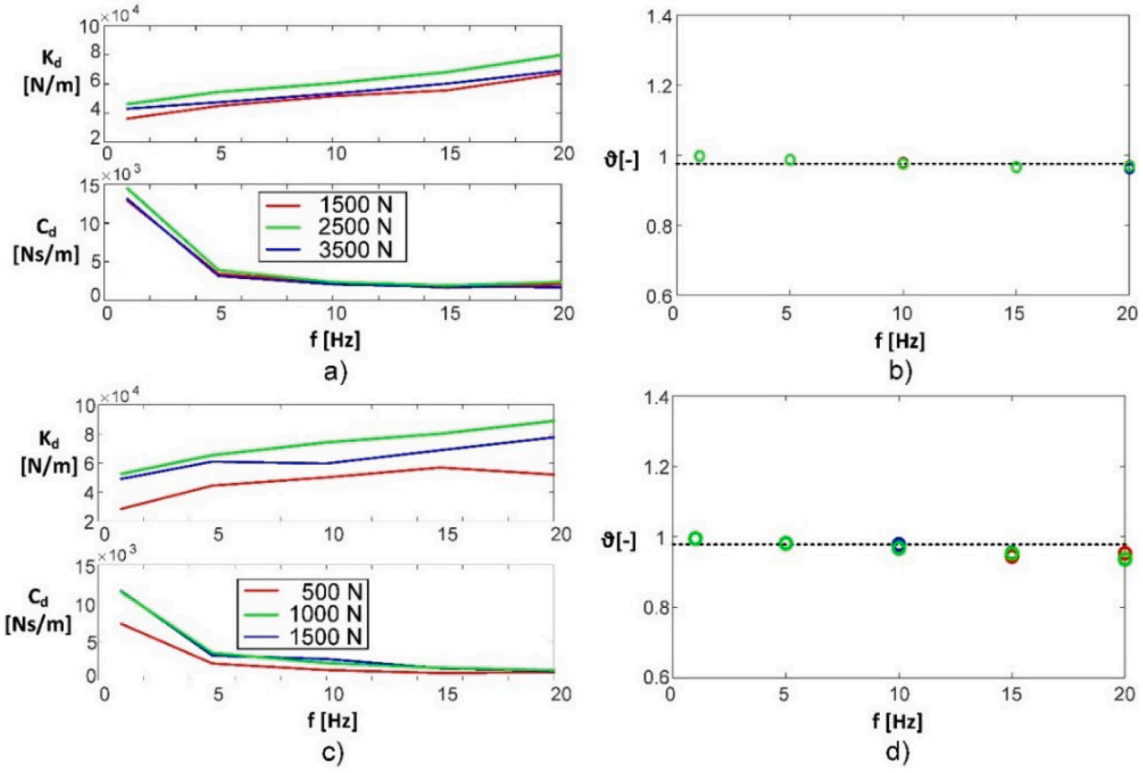

Fig. 4. Maxwell tyre model measured parameters a) 205/65 R15 tyre stiffness and damping. b) 205/65 R15 tyre viscoelastic coefficient. c) 90/58 R17 tyre stiffness and damping. d) 90/58 R17 tyre viscoelastic coefficient.

Where:.$v = \left(\dot{x}_s - \dot{x}_t\right)$

Tests were carried out on the suspension bench to verify the importance of the tyre model in the identification of the suspension system parameters and the characteristic curve of the shock absorber. The displacements of the sprung and unsprung masses were measured. In addition, the displacement of the plate exciting the system was also obtained. With these data and using the scheme of Fig. 2, the following results were obtained (see Fig. 6). Three cases were compared. Case 1: the tyre is modelled using the Maxwell model in Fig. 6a [22–23]. Case 2: a Kelvin-Voigt model is used to reproduce tyre behaviour in Fig. 6 b [22]. Case 3: a constant stiffness in the tyre is taken into account in Fig. 6c [7]. In all the figures, the experimental data representing the characteristic curve of the shock absorber, a motorcycle fork in this test, have been represented. These data have been adjusted to an experimental curve and checked against the curve obtained with points $\left\{C_a^1 \cdots C_a^{20}\right\}$ (see Table 2) and the model described in equation (6).

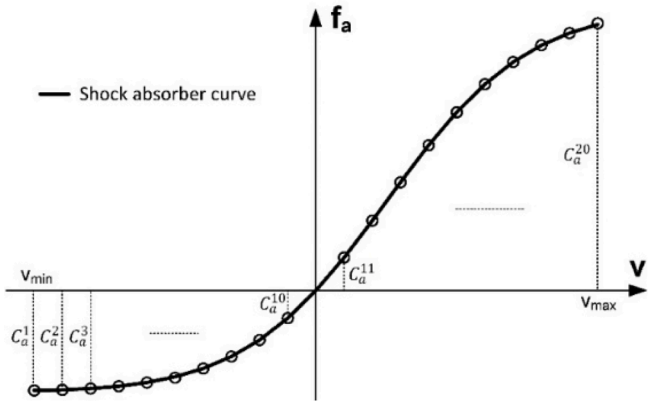

Fig. 5. Modelling of the damper characteristic curve.

As it can be seen in Fig. 6a, the data that best fit the real curve of the shock absorber are those obtained using the Maxwell tyre model. This curve is suitable for all excitation values of the unsprung mass. On the other hand, when using a Kelvin-Voigt tyre model (Fig. 6b), the data do not adequately fit the real curve when the tyre or unsprung mass is excited at high speeds, but it seems to be

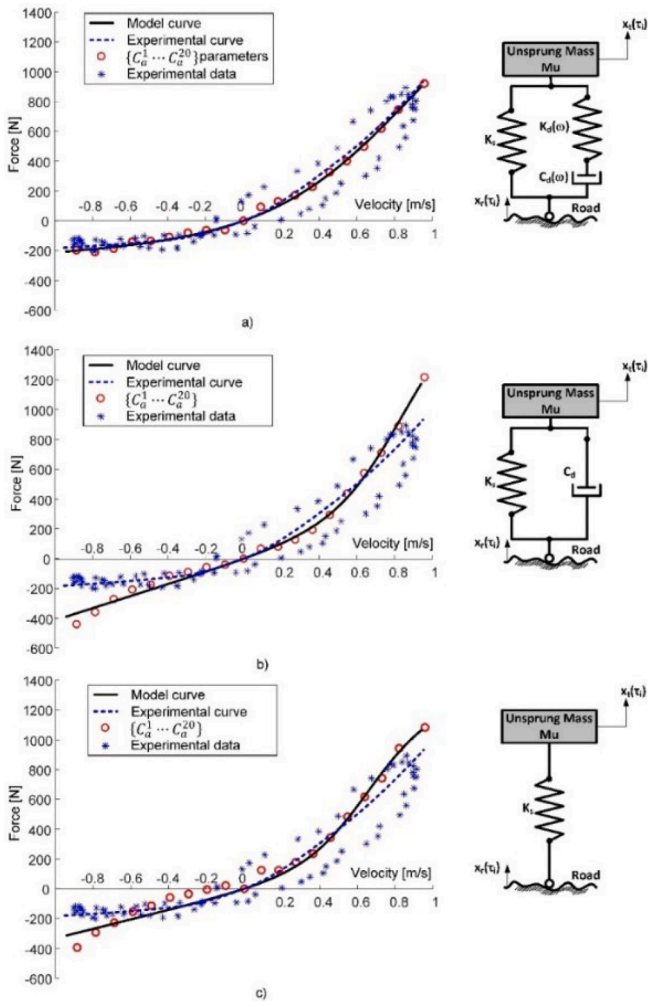

Fig. 6. Tests to obtain shock absorber characteristic curve with different tyre models. a) Maxwell model. b) Kelvin-Voigt model. c) Constant stiffness model.

adequate at low speeds. In the case of modelling the tyre only with a constant stiffness (Fig. 6c), the results obtained are poor and a clear deviation from the estimated data is observed at both high and low speeds.

Table 3 shows the values of the hyperbolic tangent curve parameters of the shock absorber model used in equation (6).

In order to highlight the importance of using an appropriate tyre model, tests were carried out using a suspension tester [12]. To this end, the suspension system (x_r) was excited with a harmonic signal with an amplitude of 4 mm and a variable frequency from 0 to 20 Hz to evaluate the entire working range of the shock absorber. The displacements of the sprung (x_s) and unsprung (x_t) mass were measured. The values of these displacements were compared with simulations obtained with different tyre models and the adjusted damping curve obtained in Table 2. Results of this comparison are included in Fig. 7. First, it can be seen that the displacements of the sprung and unsprung masses are very similar to the experimental values (Fig. 7a) when the damping characteristic curve obtained with the Maxwell model (Table 2, column 1) and the Maxwell tyre model with constant parameters $K_s = 101018$ N/m, $C_d = 1700$ Ns/m and ϑ=0.97 are used. On the other hand, worse results are obtained in the case of using the Kelvin-Voigt model with $K_s = 101018$ N/m and $C_d = 51$ Ns/m (Fig. 7b) and the model with only elastic stiffness in the tyre with $K_s = 101018$ N/m (Fig. 7c). In both cases, the displacement of the suspended mass (x_s) diverges considerably from the experimental results at high frequencies. Finally, a simulation was also conducted using the damping characteristic curve obtained utilizing the Kelvin-Voigt tyre model (Table 2, column 2) and parameters K_s and C_d of this model (Fig. 7d). In this case, it can be observed that the error is higher due to an erroneous characterization of both the shock absorber and tyre.

3. Considerations about the acceptance and rejection criteria of the suspension system in technical inspections of vehicles

Vehicle suspension system performance is regularly examined during the technical inspection of vehicles to detect faulty conditions that will compromise safety and handling. To this end, a vibrating platform test bench is commonly used in most cases. There are systems based on the measurement of the force or the displacemsent of the platform. The result of the test depends on the relationship between the maximum measured amplitude and the static value. In some cases, the difference between the values measured on both wheels of the same axle is also evaluated in these tests. However, the test method and validation criteria are not fully adequate and can lead to incorrect inspection results.

The damper ratio (ξ) previously adopted by other authors to determine a criterion for determining the suitability of a shock absorber in vehicle inspection services is evaluated next [19–21]. For this purpose, the tyre modelling described above was used and the damper ratio was determined as a function of the static force in the tyre divided by the minimum force found in the test (see Fig. 8). As it can be seen, the criteria that Calvo et al. [19] established to determine when a shock was working properly ($\xi_{limit} < 0.12$) can be different depending on the tyre model used. For example, Fig. 8a represents the curves of the Maxwell, Kelvin-Voigt and constant stiffness tyre models. In this figure, the tyre stiffness for the models described above has been set constant at the working point of the tyre, except for the Maxwell (MX) model where the real stiffness curve of the tyre has been taken into account. The difference between the Kelvin-Voigt model, constant stiffness models and the Maxwell model can be observed. Similarly, in Fig. 8b, the curves of the previous models have been plotted, but in this case, the tyre stiffness has been calculated at the beginning of the real force–displacement curve. In addition, the representation of the previous Maxwell (MX) model has been left. A difference in efficacy is again observed for the criterion established by Calvo et al. [19].

Table 2
Damper characteristic curve model parameters.

	Maxwell [N]	Kevin-Voigt [N]	Constant Stiffness [N]
C_a^1	−196.8	−439.4	−394.4
C_a^2	−208.6	−358.0	−293.2
C_a^3	−186.0	−271.0	−228.0
C_a^4	−141.8	−206.8	−154.2
C_a^5	−135.6	−173.2	−113.6
C_a^6	−108.8	−114.6	−58.6
C_a^7	−80.4	−89.0	−35.2
C_a^8	−63.2	−56.8	−5.4
C_a^9	−61.6	−39.8	21.4
C_a^{10}	0	0	0
C_a^{11}	92.8	67.6	124.6
C_a^{12}	129.6	81.0	123.8
C_a^{13}	170.8	128.0	178.0
C_a^{14}	228.2	193.6	235.4
C_a^{15}	326.8	293.8	342.6
C_a^{16}	401.0	437.0	483.0
C_a^{17}	497.8	574.4	616.8
C_a^{18}	618.4	711.0	742.2
C_a^{19}	746.2	889.6	942.0
C_a^{20}	920.4	1217.4	10821.8

Table 3
Hyperbolic tangent shock absorber model parameters.

Model	c_s [Ns/m]	K [N]	μ [s/m]	β [-]
Maxwell	68.647	937.67	1.336	−1.203
K-V	403.53	620.82	2.893	−2.418
K_{const}	315.94	461.09	3.063	−2.009

4. Experimental determination of the suspension parameters in a vehicle

In this section, the methodology developed to obtain the characteristic curves of the suspension system is applied to a real vehicle. Fig. 9a shows the test vehicle and the measurement system developed. This system is composed of four OMRON ZX-LD40 and ZX-LD100 laser sensors, with measuring ranges of 80 mm and 20 mm. These sensors measure the displacement of the sprung and unsprung masses on each side of the vehicle. For the calculation of the suspension parameters, a model of the front axle of the vehicle has been developed, which includes the modelling of the anti-roll bar and tyre using the Maxwell model (see Fig. 9b).

The equations that model the behaviour of the vehicle in this case are:

$$M_u^l \bullet \ddot{x}_t^l + K_a^l \bullet \left(x_t^l - x_s^l\right) + C_a^l \bullet \left(\dot{x}_t^l - \dot{x}_s^l\right) + K_s^l \bullet \left(x_t^l - x_r^l\right) + f_v^l + K_e\left(x_t^l - x_t^r\right) = 0 \tag{11}$$

$$M_u^r \bullet \ddot{x}_t^r + K_a^r \bullet \left(x_t^r - x_s^r\right) + C_a^r \bullet \left(\dot{x}_t^r - \dot{x}_s^r\right) + K_s^r \bullet \left(x_t^r - x_r^r\right) + f_v^r - K_e\left(x_t^l - x_t^r\right) = 0 \tag{12}$$

$$M_s \bullet \ddot{x}_G - K_a^l \bullet \left(x_t^l - x_s^l\right) - C_a^l \bullet \left(\dot{x}_t^l - \dot{x}_s^l\right) - K_a^r \bullet \left(x_t^r - x_s^r\right) - C_a^r \bullet \left(\dot{x}_t^r - \dot{x}_s^r\right) = 0 \tag{13}$$

$$I \bullet \ddot{\theta} - K_a^l \bullet \frac{b}{2}\left(x_t^l - x_s^l\right) - C_a^l \bullet \frac{b}{2}\left(\dot{x}_t^l - \dot{x}_s^l\right) + K_a^r \bullet \frac{b}{2}\left(x_t^r - x_s^r\right) + C_a^r \bullet \frac{b}{2}\left(\dot{x}_t^r - \dot{x}_s^r\right) = 0 \tag{14}$$

Where f_v^l and f_v^r, are the viscoelastic forces in each element of the Maxwell model of the left and right tyre, which are modelled according to equation (4), K_e is the stiffness of the anti-roll bar, b is the track of the vehicle and I is the moment of inertia. Finally, x_G and θ are defined according to the following equations:

$$x_G = \frac{x_s^l + x_s^r}{2} \tag{15}$$

$$\theta = arctg\left(\frac{x_s^l - x_s^r}{b}\right) \tag{16}$$

In this case the objective function is defined as:

$$\begin{aligned} &min\left[\sum\nolimits_{i=0}^{nsample} \frac{\sqrt{\left\{f_1(\chi,\tau_i)^2 + f_2(\chi,\tau_i)^2 + f_3(\chi,\tau_i)^2 + f_4(\chi,\tau_i)^2\right\}}}{nsample}\right] \\ &subjectto: \left\{\begin{array}{c} \chi(1) + \chi(2) + \chi(3) = M_{1/2} \\ \chi(2) = \chi(3) \end{array}\right\} \end{aligned} \tag{17}$$

Where the vector of design variables corresponds to equation (17) and functions f_1,f_2, f_3 and f_4 are obtained by introducing the measurements and design variables in equations (11), (12), (13) and (14) respectively.

It should be noted that in the experimental test, the exciter plate does not cause high speed values in the damper. Therefore, the curve that models the behaviour of the shock absorber is composed of 10 points, which are enough to evaluate the performance of the damper in that working range.

Fig. 10 shows the curves obtained by the algorithm. The values provided by the optimization algorithm are included in Table 4. It can be seen that the curves obtained are properly adjusted to the real curves of the vehicle's shock absorbers. Force-velocity and force–displacement characteristic curves of the shock absorbers were obtained using a suspension test bench [12]. Forces and displacements were measured using high-precision load cells and laser sensors respectively. In this case, although the shock absorbers were new, the left and right shock absorbers did not behave in the same way. It is noteworthy that the proposed method is capable of detecting these differences in the behaviour of each of the shock absorbers. For the experimental tests, a commercial plate bench has been used. As previously indicated, the system does not allow the shock absorbers to be excited over their entire operating range. For this reason, the curves obtained by the algorithm only comprise a velocity range between −0.4 to 0.4 m/s.

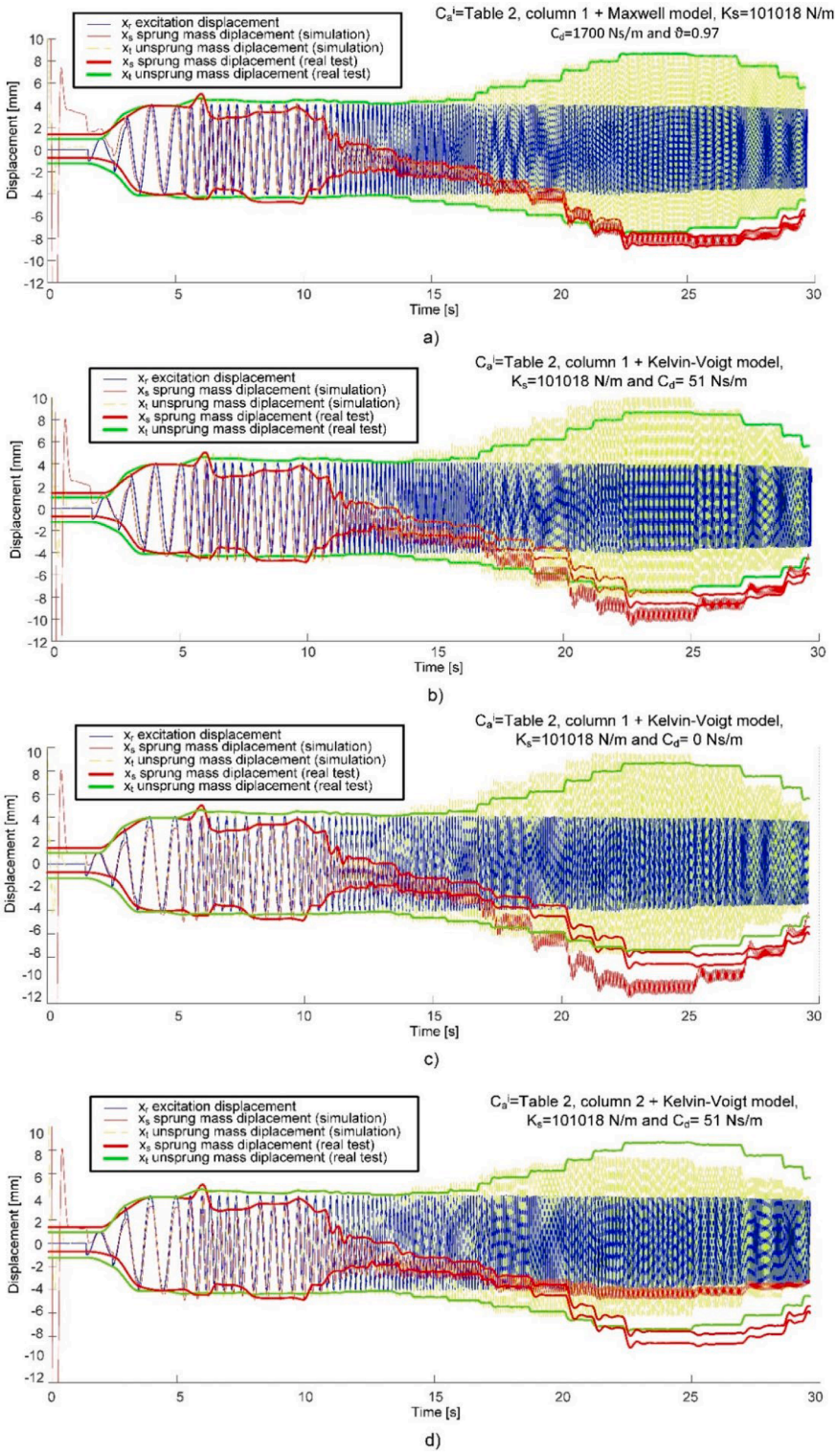

Fig. 7. Real test and simulation comparation between several tyre models.

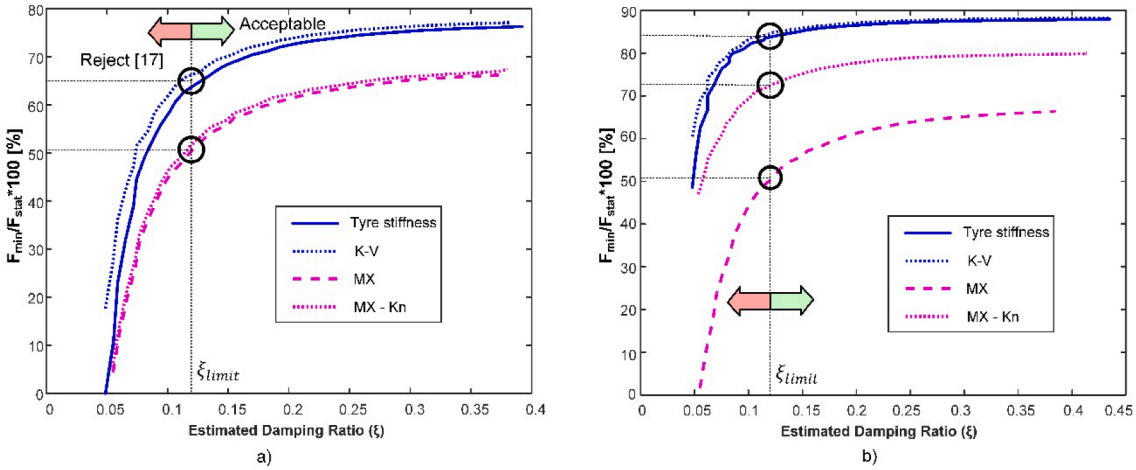

Fig. 8. EUSAMA versus Damping ratio cuves. a) Tyre stiffness at working point. b) Tyre stiffness at origin.

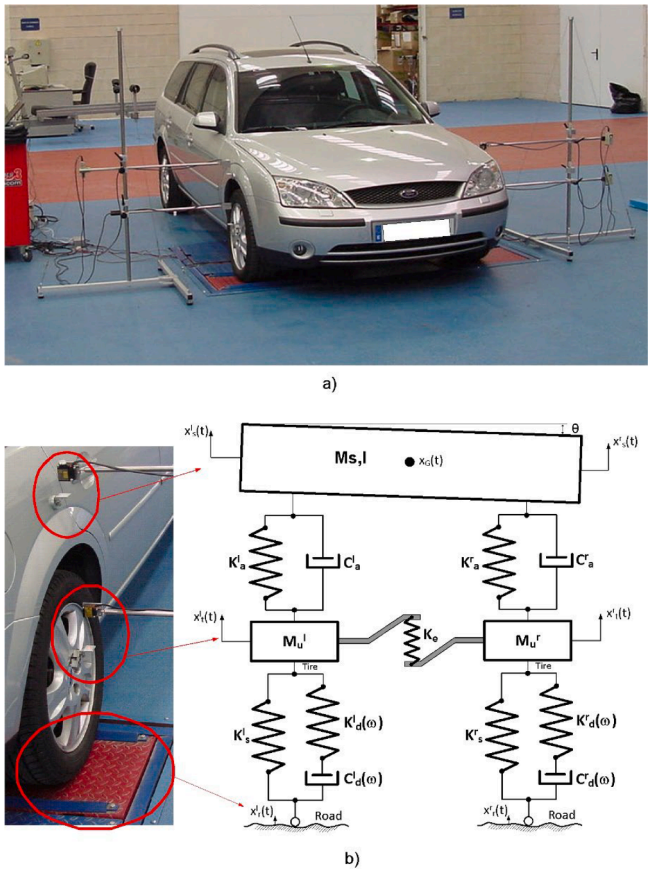

Fig. 9. (a) Test vehicle (b) Model of front axle used.

5. Conclusions

In this work, a novel methodology has been proposed to determine the characteristic curves of a shock absorber without dismounting it from the vehicle. To this end, the importance of the tyre model has been studied in order to be able to evaluate the behaviour of the shock absorber accurately. It has been found that a tyre model capable of reproducing the viscoelastic behaviour of the tyre faithfully is necessary. A realistic tyre model is required to obtain robust estimates of the characteristic curves of the shock

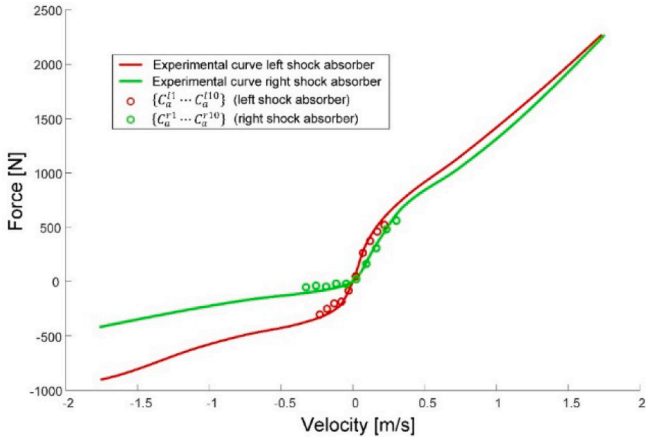

Fig. 10. Characteristic curve of the real shock absorber and the one obtained by the proposed method.

Table 4
Right and left shock absorber model parameters.

C_a^{r1}	−51.69 N	C_a^{l1}	−302.97 N
C_a^{r2}	−38.27 N	C_a^{l2}	−250.02 N
C_a^{r3}	−46–42 N	C_a^{l3}	−200.92 N
C_a^{r4}	−19.25 N	C_a^{l4}	−184.69 N
C_a^{r5}	−19.93 N	C_a^{l5}	−83.47 N
C_a^{r6}	25.05 N	C_a^{l6}	48.46 N
C_a^{r7}	163.49 N	C_a^{l7}	264.36 N
C_a^{r8}	307.88 N	C_a^{l8}	373.51 N
C_a^{r9}	481.64 N	C_a^{l9}	460.38 N
C_a^{r10}	561.50 N	C_a^{l10}	520.08 N

absorber, especially at high frequencies.

Once a more accurate model of the suspension system of a vehicle is used, an optimization process using evolutionary algorithms is carried out to determine the characteristic curve of the shock absorber. The measurement of the displacements of the sprung and unsprung masses and the excitation of the system are used as inputs to the algorithm. Tests carried out on an experimental vehicle have demonstrated that the proposed methodology is capable of obtaining the characteristic curves of the shock absorbers, being able to detect small differences that exist between the right and left shock absorbers.

Funding: This work was supported in part by the Spanish Innovation Science Ministry under Grant PID2019-105572RB-I00.

Declaration of Competing Interest

The authors declare the following financial interests/personal relationships which may be considered as potential competing interests: Juan A. Cabrera reports financial support was provided by Spanish Innovation Science Ministry.

Data availability

No data was used for the research described in the article.

References

[1] Guba S, Ko Y, Rizzoni G, et al. The Impact of Worn Shocks on Vehicle Handling and Stability. SAE Technical Paper Series. doi:10.4271/2006-01-0563.
[2] J.A. Calvo, V. Díaz, J.L. San Román, D. García-Pozuelo, Influence of shock absorber wearing on vehicle brake performance, Int. J. Automotive Technol. 9 (4) (2008) 467–472.
[3] P. Kubo, C. Paiva, A. Ferreira, et al., Influence of shock absorber condition on pavement fatigue using relative damage concept, J. Traffic Transp. Eng. 2 (2014) 406–413.
[4] H. Koylu, A. Cinar, Dynamical investigation of effects of variable damper settings induced brake pressure oscillations on axle and wheel oscillations during ABS-braking based on experimental study, Meccanica 48 (5) (2013) 1093–1115.
[5] A.G. Gracia, F. Jimenez, J. Paez, A. Narvaez, Theoretical and experimental analysis to determine the influence of the ageing process of the shock-absorber on safety, Int. J. Vehicle Design 40 (1/2/3) (2006) 15.
[6] M.D. Bedük, K. Çalışkan, R. Henze, F. Küçükay, Effects of damper failure on vehicle stability, Proc. IMechE Part D: J. Automobile Eng. 227 (7) (2013) 1024–1039.
[7] R.N. Jazar, Vehicle Dynamics: Theory and Application, New York, NY, Springer, USA, 2017.

[8] H. Pang, X.u. Zhang, J. Chen, K. Liu, Design of a coordinated adaptive backstepping tracking control for nonlinear uncertain active suspension system, Appl. Math. Model. 76 (2019) 479–494.
[9] H. Pang, F. Liu, Z. Xu, Variable universe fuzzy control for vehicle semi-active suspension system with MR damper combining fuzzy neural network and particle swarm optimization, Neurocomputing 306 (2018) 130–140.
[10] A. Simms, D. Crolla, The Influence of Damper Properties on Vehicle Dynamic Behaviour. SAE paper 2002-01-0319, 2002.
[11] V.V. Novikov, A.V. Pozdeev, A.S. Diakov, Research and testing complex for analysis of vehicle suspension units, Procedia Eng. 219 (2015) 465–470.
[12] E.C. Acosta, J.J.C. Aguilar, J.A.C. Carrillo, J.M.V. Garcia, J.P. Fernandez, M.G.A. Vargas, Modeling of tire vertical behavior using a test bench, IEEE Access 8 (2020) 106531–106541.
[13] R.K. Taylor, L.L. Bashford, M.D. Schrock, Methods for measuring vertical tire stiffness, Trans. ASAE 43 (6) (2000) 1415–1419.
[14] S.h. Lajqi, J. Gugler, N. Lajqi, A. Shala, R. Likaj, Possible experimental method to determine the suspension parameters in a simplified model of a passenger car, Int. J. Automot. Technol. 13 (4) (2012) 615–621.
[15] H. Nozaki, Y. Inagaki, Technology for measuring and diagnosing the damping force of shock absorbers and the constant of coil springs when mounted on a vehicle, JSAE Review 20 (1999) 413–419.
[16] R. Isermann, Diagnosis Methods for Electronic Controlled Vehicles, Veh. Syst. Dyn. 36 (2-3) (2001) 77–117.
[17] D. Fischer, R. Isermann, Mechatronic semi-active and active vehicle suspensions, Control Eng. Pract. 12 (11) (2004) 1353–1367.
[18] W. Schiehlen, B. Hu, Spectral simulation and shock absorber identification, Int. J. Non Linear Mech. 38 (2) (2003) 161–171.
[19] J.A. Calvo, V. Diaz, J.L. San Roman, Establishing inspection criteria to verify the dynamic behaviour of the vehicle suspension system by a platform vibrating test bench, Int. J. Vehicle Design 38 (2005) 290–306.
[20] J.A. Calvo, J.L. San Roman, C. Alvarez-Caldas, Procedure to verify the suspension system on periodical motor vehicle inspection, Int. J. Vehicle Design 63 (2013) 1–17.
[21] M. Klapka, I. Mazůrek, O. Macháček, M. Kubík, Twilight of the EUSAMA diagnostic methodology, Meccanica 52 (9) (2017) 2023–2034.
[22] J. Lemaitre, Handbook of Materials Behavior Models, Academic, Cambridge, MA, USA, 2001.
[23] A. Hackl, W. Hirschberg, C. Lex, et al., Parametrisation of a Maxwell model for transient tyre forces by means of an extended firefly algorithm, Adv. Mech. Eng. 9 (2016) 1–11.
[24] R. Storn, K. Price, Differential evolution. A simple and efficient heuristic scheme for global optimization over continuous spaces, J. Global Optimization 11 (1997) 341–359.
[25] N.M. Kwok, Q.P. Ha, T.H. Nguyen, J. Li, B. Samali, A novel hysteretic model for magnetorheological fluid dampers and parameter identification using particle swarm optimization, Sensor Actuator 132 (2) (2006) 441–451.